

COMPARATIVE MAGNETIC RESONANCE IMAGING FINDINGS BETWEEN GLIOMAS AND PRESUMED CEREBROVASCULAR ACCIDENTS IN DOGS

VICENTE CERVERA, WILFRIED MAI, CHARLES H. VITE, VICTORIA JOHNSON, BETSY DAYRELL-HART,
GABRIELA S. SEILER

Cerebrovascular accidents, or strokes, and gliomas are common intraaxial brain lesions in dogs. An accurate differentiation of these two lesions is necessary for prognosis and treatment decisions. The magnetic resonance (MR) imaging characteristics of 21 dogs with a presumed cerebrovascular accident and 17 with a glioma were compared. MR imaging findings were reviewed retrospectively by three observers unaware of the final diagnosis. Statistically significant differences between the appearance of gliomas and cerebrovascular accidents were identified based on lesion location, size, mass effect, perilesional edema, and appearance of the apparent diffusion coefficient map. Gliomas were predominantly located in the cerebrum (76%) compared with presumed cerebrovascular accidents that were located mainly in the cerebellum, thalamus, caudate nucleus, midbrain, and brainstem (76%). Gliomas were significantly larger compared with presumed cerebrovascular accidents and more commonly associated with mass effect and perilesional edema. Wedge-shaped lesions were seen only in 19% of presumed cerebrovascular accidents. Between the three observers, 10–47% of the presumed cerebrovascular accidents were misdiagnosed as gliomas, and 0–12% of the gliomas were misdiagnosed as cerebrovascular accidents. Diffusion weighted imaging increased the accuracy of the diagnosis for both lesions. Agreement between observers was moderate ($\kappa = 0.48$, $P < 0.01$). © 2010 *Veterinary Radiology & Ultrasound*, Vol. 52, No. 1, 2011, pp 33–40.

Key words: cerebrovascular accident, dog, glioma, MRI.

Introduction

MAGNETIC RESONANCE (MR) IMAGING characteristics of glial tumors and cerebrovascular accident in animals have been described.^{1–8} Gliomas are the most common canine intraaxial brain tumors and the second most frequent canine brain tumor after meningiomas.³ According to the most recent Veterinary World Health Organization classification for central nervous system tumors, gliomas are divided into astrocytic tumors, oligodendroglial tumors, ependymal tumors, and other gliomas.⁹ On MR imaging, canine gliomas are typically hypointense and heterogeneous on T1-weighted (T1W) images, hyperintense, and heterogeneous on T2-weighted (T2W) images and proton density-weighted images, with significant mass effect and perilesional edema. The major-

ity of gliomas are located in the cerebrum and diencephalon and less commonly in the cerebellum.^{1,2,10} Contrast enhancement is variable, ranging from none to variably intense nonuniform or ring-like enhancement.²

Cerebrovascular accident is characterized by a sudden onset of nonprogressive focal brain signs secondary to cerebrovascular disease.⁴ Clinical signs are always acute with no progression or improvement after a short period of time. Cerebrovascular accidents are broadly divided in two groups: ischemic and hemorrhagic. Ischemic cerebrovascular accidents are the result of the disturbance to the arterial supply or venous drainage caused by a thrombus, embolus, or secondary to blood vessel abnormalities or severe hypoperfusion. Ischemic cerebrovascular accidents can be subdivided into nonhemorrhagic infarcts and hemorrhagic infarcts. Hemorrhage secondary to infarction is believed to occur when a vessel reperfuses in presence of a postinfarcted damaged endothelium after a part of the embolus lyses or migrates. On the other hand, hemorrhagic cerebrovascular accident is usually secondary to hypertension or aneurysm rupture.^{5,11–14} As in humans, the majority of canine cerebrovascular accidents are ischemic.^{4,5} Cerebrovascular accidents have been characterized traditionally as being wedge shaped with minimal mass effect and located predominantly in the cerebellum, thalamus and midbrain, and rarely within the cerebrum.^{4–7,11} They are usually homogeneous and hypo-

From the Department of Clinical Studies-Philadelphia, School of Veterinary Medicine, University of Pennsylvania, 3900 Delancey Street, Philadelphia, PA 19104-6010 (Cervera, Mai, Vite), Vet CT Specialists Ltd, 16 Covent Garden, Cambridge CB1 2HR, UK (Johnson), South Paws Veterinary Specialists, 8500 Arlington Blvd, Fairfax, VA 22031 (Dayrell-Hart), and the Department of Molecular Biomedical Sciences, North Carolina State University, 4700 Hillsborough Street, Raleigh, NC 27606 (Seiler).

Results of this study were presented at the 2009 annual scientific meeting of the ACVR in Memphis, Tennessee.

Address correspondence and reprint requests to Dr. Gabriela S. Seiler, at the above address. E-mail: gsseiler@ncsu.edu

Received April 19, 2010; accepted for publication July 18, 2010.

doi: 10.1111/j.1740-8261.2010.01749.x

intense on T1W images and hyperintense on T2W images with the presence and degree of contrast enhancement dependent on the time of imaging after the ischemic event. Contrast enhancement may be present at 24–48 h postinfarction, but is usually more evident 1–8 weeks postinfarction.^{4,5,11,12}

Cerebrovascular accidents and gliomas may produce acute neurologic dysfunction that may include, but is not limited to, seizures, mentation change, and vision loss.^{3,11} Therefore, an accurate differentiation between the two lesions by imaging would be important for prognosis and appropriate treatment. However, there is some overlap in the appearance of the two lesions in MR images. For example, in dogs with histologically confirmed intracranial tumors, one out of 15 gliomas was misdiagnosed as a hemorrhagic infarct.¹⁵ Our purpose was to compare the MR imaging characteristics of canine gliomas and presumed cerebrovascular accidents.

Materials and Methods

The histopathology database from 1997 to 2009 was searched for dogs with a diagnosis of cerebrovascular accident or glioma, excluding ependymoma. Of these dogs, those having a brain MR imaging study within 30 days before the histopathologic diagnosis were selected. Additionally, the patient database of two hospitals (University of Pennsylvania, South Paws) was searched for dogs with intraaxial lesions, where the differential diagnosis included presumed cerebrovascular accident or glioma. Of these dogs, those alive 1 year after imaging with improvement or lack of progression of the clinical signs were included as presumed cerebrovascular accidents. These steps resulted in a population of 38 dogs (Table 1). Of this group, three dogs were treated with corticosteroids, two of them for 2 weeks, and one for 3 months.

Imaging was performed in all dogs using one of two 1.5 T MR units (Signa 1.5 T, GE Medical Systems, Milwaukee, WI; Siemens Symphony 1.5 T, Aurora, OH). Imaging protocols varied between patients. T1W images (T1W, TR = 400–766 ms, TE = 9–12 ms) and T2W images (T2W, TR = 3500–6600 ms, TE = 9–81 ms) were available in all dogs. Gadolinium* was administered intravenously in all dogs (0.2 ml/kg) and T1W postcontrast images (TR = 416–766 ms, TE = 9–10 ms) were acquired. Diffusion-weighted images with a b-value of 1000 (DWI, TR = 10,000 ms, TE = 80–88 ms), and apparent diffusion coefficient (ADC) maps were available in 16 dogs, nine with presumed cerebrovascular accidents, and seven with gliomas.

All images were reviewed by two board-certified radiologists and one board-certified neurologist who were unaware of the final diagnosis. Observers were aware that all

dogs had either a glioma or a cerebrovascular accident. Reviewers evaluated the following characteristics of the lesion in the MR images: location, shape, size (defined as the maximum dimension in any direction), mass effect, perilesional edema, margin definition, signal intensity on T1W pre- and postcontrast, T2W, DWI images and on ADC maps (when available), signal regularity (homogeneous or heterogeneous), and intensity and type of contrast enhancement. Presence of mineralization, hemorrhage, cysts, loss of brain volume, ventricular enlargement, transtentorial herniation, and cerebellar herniation were also assessed. Mineralization was defined as a hypointense or hyperintense signal on T1W images and hypointense signal on T2W images. Hemorrhage was divided into subacute hemorrhage, defined as a hyperintense lesion on T1W images and hypo or hyperintense lesion on T2W images, and chronic hemorrhage, defined as iso- to slightly hypointense lesion on T1W images and hypointense lesion on T2W images. Reviewers were also asked to make a diagnosis of glioma, cerebrovascular accident, or undecided. This decision was made based on the imaging characteristics of these lesions as described in the literature and individual experience, as would happen in clinical practice.

All statistical analyses were performed using Microsoft® Office Excel 2003† for Windows and available online resources.¹⁶ A *P*-value of <0.05 was considered statistically significant. For categorical (descriptive) variables, a consensus opinion of all reviewers was sought that would best describe the imaging appearance of a lesion. Categorical variables were compared using the chi-square test, where appropriate. Numerical variables (age, time from the onset of clinical signs to MR imaging, time from the MR imaging study to the final diagnosis, and size of the lesions) were described using the median and range, and gliomas and presumptive cerebrovascular accidents were compared using a Fisher's exact test. A consensus was not formed for diagnosis, to evaluate the range of diagnostic accuracy. κ agreement coefficient was calculated for the final diagnosis of the lesions between the observers.

Results

All dogs had a single lesion. Twenty-one dogs had presumed cerebrovascular accidents. In four, the diagnosis was confirmed histopathologically (three ischemic and one hemorrhagic) and in the other 17, the diagnosis of cerebrovascular accident was based on clinical outcome, as described above. A definitive histopathologic diagnosis was available for all dogs with glioma: 10 were oligodendrogliomas, two were noncategorized gliomas, two were astrocytomas, and there was one each mixed glioma, glioblastoma multiforme, and gliomatosis cerebri.

*Magnevist, Berlex Imaging, Wayne, NJ.

†Microsoft Excel, Microsoft Corp., Redmond, WA.

TABLE 1. Age, Gender and Breed Distribution of Dogs Diagnosed with Either Presumed CVA or Glioma

	Presumed CVA (<i>n</i> = 21)	Gliomas (<i>n</i> = 17)
Median Age (Range) (Years)	8 (2–19)	9 (5–14)
Gender	10 males, 11 females	Three males, 14 females
Breed	Mixed breed (four), Golden Retriever (three), Labrador (two), Boxer (two), Poodle (one), Miniature Schnauzer (one), Bulldog (one), Shar Pei (one), Rottweiler (one), Jack Russell Terrier (one), English Setter (one), Shih-Tzu (one), Weimaraner (one), and American Eskimo (one)	Boxer (eight), Mixed Breed (three), French Bulldog (two), Labrador (two), American Bulldog (one), and Standard poodle (one)

CVA, cerebrovascular accident.

Boxers and females were overrepresented in the glioma group ($P < 0.001$ and < 0.05 , respectively, Table 1). Statistically significant MR image findings were as follows: mass effect and perilesional edema were more common in gliomas (100 and 88%, respectively) than in presumed cerebrovascular accidents (24 and 19%, respectively) ($P < 0.001$); presumed cerebrovascular accidents were significantly smaller (12 mm, range 3–30 mm) than gliomas (23 mm, range 12–40 mm) ($P < 0.01$); cerebral location was significantly more common for gliomas ($P < 0.01$), with 13 gliomas located in the cerebrum, three in the caudate nucleus, and one in the midbrain. Presumed cerebrovascular accidents were located as follows: five in the cerebrum, three in the caudate nucleus, four in the thalamus, two in the midbrain, one in the brainstem, and six in the cerebellum. Differences in ADC maps were statistically significant between both lesions with the majority of gliomas being hyperintense ($P < 0.05$). Wedge-shaped lesions were seen only with presumed cerebrovascular accidents (19%) and never with gliomas. No statistically significant difference was found between presumed cerebrovascular accidents and gliomas for any of the other imaging characteristics.

DWI was performed in nine of 21 dogs with presumed cerebrovascular accidents. Seven lesions were hyperintense in the diffusion image, one was isointense in the diffusion image, and in one there was mixed signal intensity in the diffusion image. On ADC maps, five of nine presumed cerebrovascular accidents were hypointense, three were hyperintense, and one had mixed signal intensity. DWI was performed in seven of 17 dogs with gliomas. Six tumors were hyperintense in the diffusion image and one was hypointense. On the ADC maps, six of seven tumors were hyperintense, and one had mixed signal intensity. The

difference in lesion intensity in the ADC maps was statistically significant between gliomas and presumed cerebrovascular accidents with the majority of presumed vascular lesions being hypointense and most gliomas being hyperintense ($P < 0.05$).

The diagnoses of all three observers are summarized in Table 2. Between 10 and 47% of the presumed cerebrovascular accidents were misdiagnosed as gliomas, whereas 0–12% of gliomas were misdiagnosed as cerebrovascular accidents. When DWI was added, the percentage of presumed cerebrovascular accidents misdiagnosed as gliomas decreased to 11–33% and none of the gliomas were misdiagnosed as a cerebrovascular accident. For the misdiagnosed presumed cerebrovascular accidents, there was no histopathology available. All gliomas misdiagnosed as cerebrovascular accident were oligodendrogliomas. Of the gliomas, where observers were undecided about the diagnosis, there were two oligodendrogliomas, one gliomatosis cerebri, and one noncategorized glioma. Two of the cerebrovascular accidents, where observers were undecided, were histopathologically characterized as ischemic cerebrovascular accident. Moderate agreement was found among the three observers ($\kappa = 0.48$, $P < 0.01$).

Discussion

Based on our study, it is apparent that there is some overlap between the MR imaging features of gliomas vs. presumed cerebrovascular accidents. In our patients, 10–47% of presumed cerebrovascular accidents were misdiagnosed as gliomas (Fig. 1) and 0–12% of gliomas, specifically oligodendrogliomas, were misdiagnosed as presumed cerebrovascular accidents (Fig. 2).

TABLE 2. Magnetic Resonance Imaging Diagnoses of Three Observers Compared with Final Diagnoses

Dogs	Final Diagnosis	Observer 1			Observer 2			Observer 3		
		CVA	Glioma	Undecided	CVA	Glioma	Undecided	CVA	Glioma	Undecided
All	Presumed CVA (<i>n</i> = 21)	15	5	1	9	10	2	18	2	1
All	Glioma (<i>n</i> = 17)	0	16	1	0	14	3	2	13	2
DWI	Presumed CVA (<i>n</i> = 9)	8	1	0	4	3	2	8	1	0
DWI	Glioma (<i>n</i> = 7)	0	7	0	0	6	1	0	6	1

CVA, cerebrovascular accident.

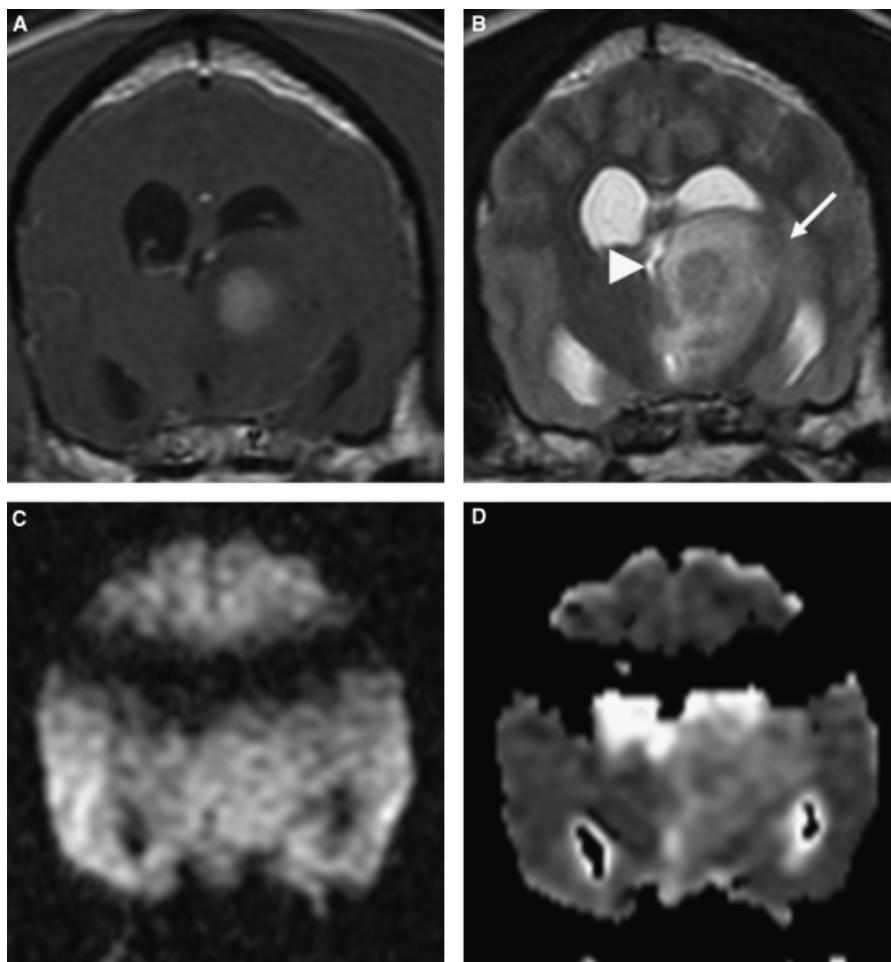


FIG. 1. (A) Transverse T1-weighted postcontrast image, (B) T2-weighted image, (C) DWI, and (D) ADC map of a dog with a presumed hemorrhagic cerebrovascular accident that was misdiagnosed as glioma based on MRI findings. (A) The mass, located in the left thalamus, strongly contrast enhances in the center in T1-weighted postcontrast images. (B) On T2-weighted images, the same central region is hypointense with a hyperintense periphery (B) likely representing marked mass effect (arrowhead) and perilesional edema (arrow). (C and D) There are mixed intensities in both the DWI and ADC map that were not helpful in distinguishing between tumor and infarct. Some of the findings that could point toward a presumed hemorrhagic cerebrovascular accident were the hypointensities seen in both T1W and T2W images with the marked contrast enhancement in the center of the lesion, explained by potential reperfusion. There is a vibration artifact in both images.

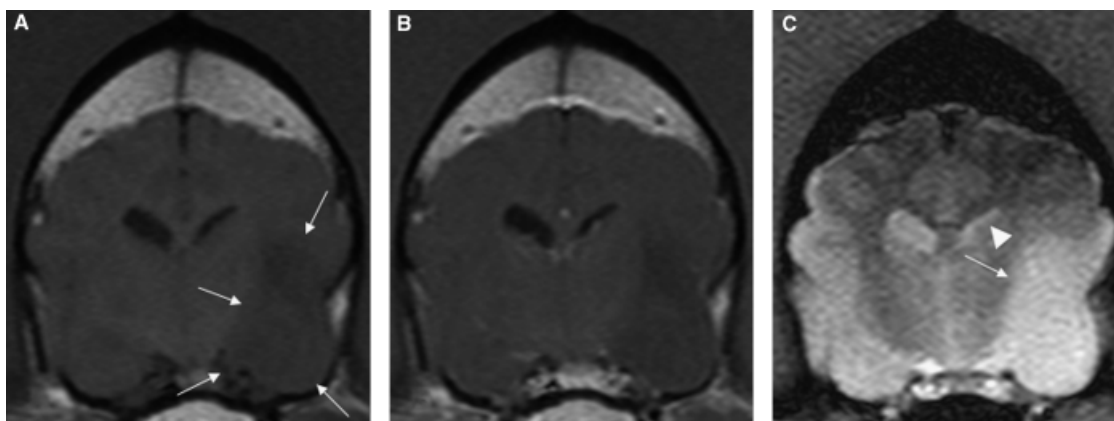


FIG. 2. (A) Transverse T1-weighted image, (B) transverse T1-weighted postcontrast image, and (C) transverse T2-weighted image of a dog with a confirmed oligodendroglioma misdiagnosed as a cerebrovascular accident. (A) The lesion (arrows) located in the left temporal lobe is irregular and hypointense on T1-weighted images, with almost no contrast enhancement (B). (C) The lesion is hyperintense on T2-weighted images, with mild mass effect as seen by the mild compression of the left lateral ventricle (arrowhead) and mild perilesional edema (arrow).

The majority of gliomas had mass effect and perilesional edema, which is consistent with the literature.^{2,4,6,7,12} However, 24% of presumed cerebrovascular accidents had mass effect and perilesional edema as well, which could lead to confusion with gliomas. Mass effect and perilesional edema are two processes intimately associated with tissue infarction. Within minutes after severe ischemia, cytotoxic edema develops. Several hours later, the blood–brain barrier starts losing its integrity. With breakdown of the blood–brain barrier, vasogenic edema ensues, becoming maximal at 3–5 days postinfarction, resulting in brain swelling and evidence of mass effect.¹⁷ This mass effect then recedes with time, hence it is suspected that an additional MR imaging examination few weeks after the initial examination may provide a clearer distinction between gliomas and vascular lesions.¹⁷

The formation of peritumoral edema in gliomas is poorly understood in humans and is presumably related to

the production of a vascular permeability factor by the neoplasm. In humans, the regions interpreted as edema on MR images are known to be a combination of tumor cells and edema on histopathology.¹⁸

Contrast enhancement was seen with similar frequency in both cerebrovascular accidents and gliomas, with variable enhancement patterns. Ring enhancement was as common in gliomas as in cerebrovascular accidents. Contrast enhancement is due to leakage of contrast medium through the damaged blood–brain barrier (Figs. 3 and 4).¹⁷ In people with brain infarction, contrast enhancement is seen after the mass effect resolves and lasts for approximately 6–8 weeks. Therefore, in people, enhancing lesions with significant mass effect are unlikely to represent cerebral infarction.¹⁷ Three dogs with a presumed cerebrovascular accident in this study had mass effect and contrast-enhancing lesions. Two of these dogs underwent MR imaging 1 day after onset of clinical signs; one of these

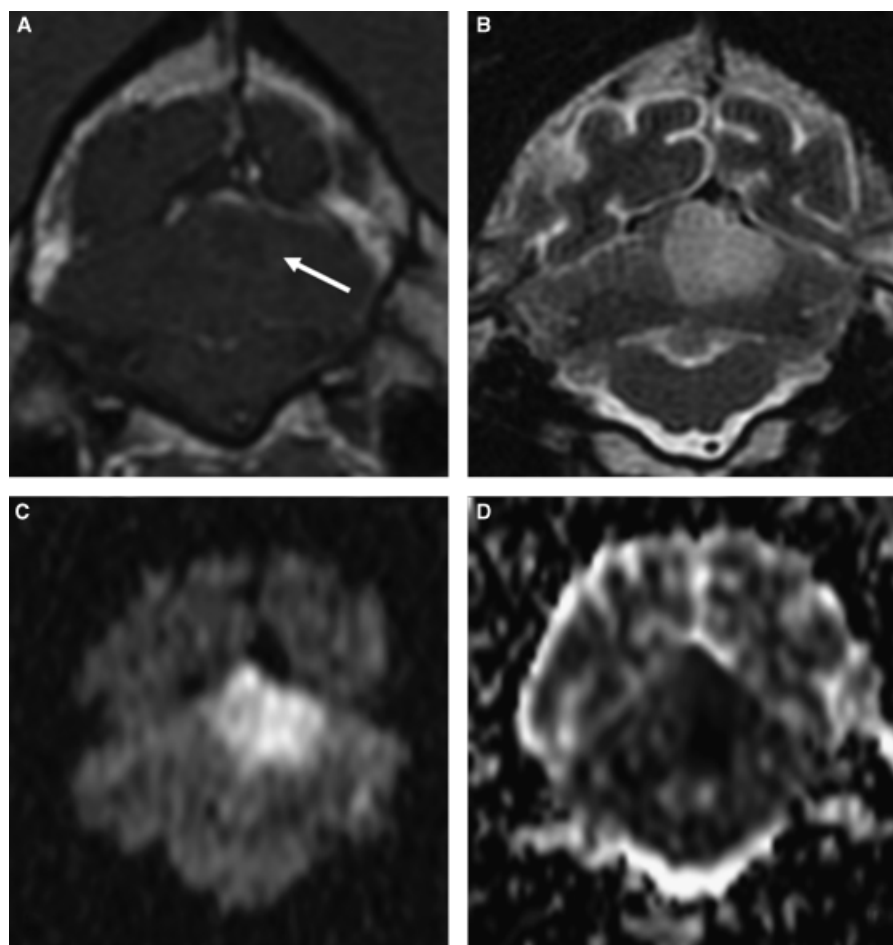


FIG. 3. (A) Transverse T1-weighted postcontrast image, (B) T2-weighted image, (C) DWI, and (D) ADC map of a dog with a presumed cerebrovascular accident. (A) The mass located in the left cerebellar hemisphere enhances very mildly (arrow) and is wedge shaped on T2-weighted images (B) with no mass effect or perilesional edema. (C and D) The lesion is hyperintense on DWI and hypointense on the ADC map, which is consistent with an acute cerebrovascular accident.

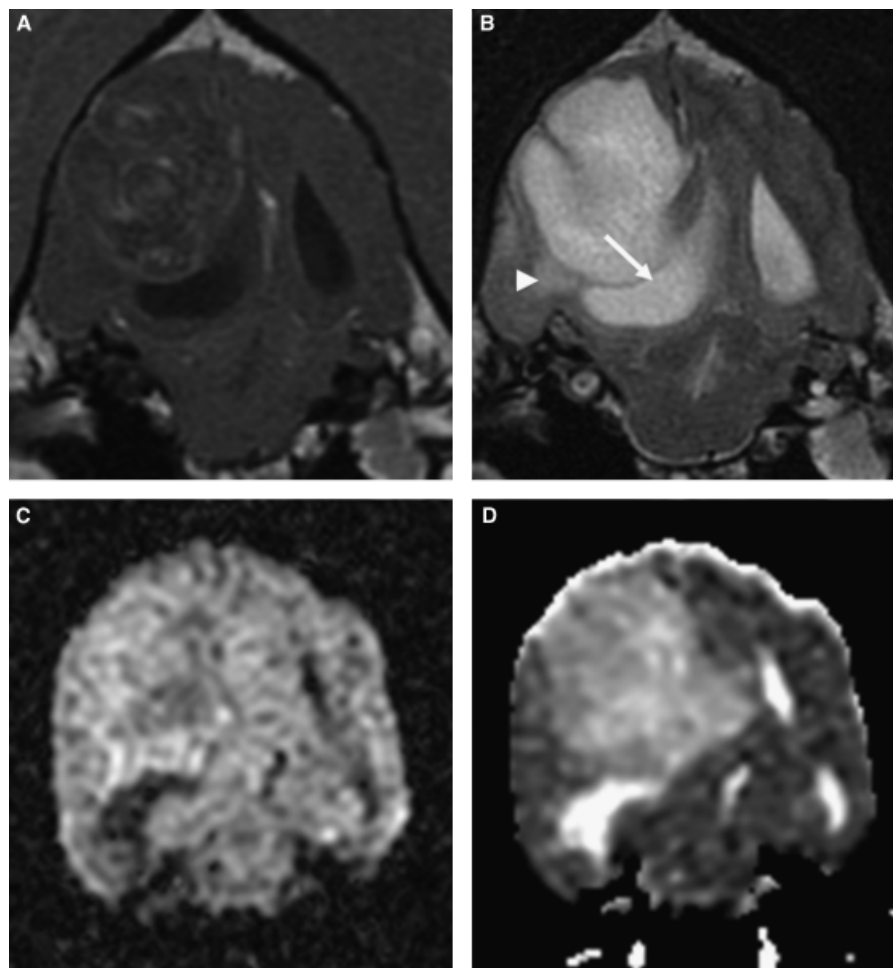


FIG. 4. (A) T1-weighted postcontrast image, (B) T2-weighted image, (C) DWI, and (D) ADC map of a dog with a confirmed glioma in the right temporal lobe. (A) The mass mildly contrast enhances. (B) Note the outward growth of the mass, producing marked mass effect and compressing the right lateral ventricle (arrow) and the perilesional edema (arrowhead) affecting both white and gray matter. (C and D) The hyperintensities in the DWI and ADC map are consistent with T2 shine-through effect.

dogs had ring enhancement and the other had marked heterogeneous contrast enhancement. It is possible that the former dog developed collateral vessels earlier, overlapping with the period of vasogenic edema, therefore developing contrast enhancement and mass effect together. The enhancement pattern in the latter dog could be due to lysis and migration of a potential embolus allowing early reperfusion and contrast medium leakage into the infarcted area. The third dog was imaged 2 weeks after onset of clinical signs, the reason the presence of both contrast enhancement and mass effect is unclear in this dog.

Presumed cerebrovascular accidents were significantly smaller than gliomas. One presumed cerebrovascular accident located in the thalamus measured 17 mm in maximum dimension. This is an unusual finding given that the thalamus is perfused by the small caudal perforating arteries which, when infarcted, give rise to lacunar infarcts.⁵ The most plausible reason for the larger size of this lesion given

the hypointensity seen in both T1W and T2W images and the marked contrast enhancement in the center of the lesion is again a hemorrhagic cerebrovascular accident due to reperfusion (Fig. 1).

Cerebral infarcts have been described as wedge shaped.^{4,7,12} In our study, the presumed cerebrovascular accidents were primarily oval or round, particularly in areas predisposed to lacunar infarcts, but round or oval lesions were also found in a few dogs in areas predisposed to territorial infarcts, such as the cerebellum. Most lacunar infarcts in humans are also oval or round.¹⁹ Based on our results, it appears that the shape of the lesion may not be a good predictor of its nature, although wedge-shaped lesions were seen only with presumed cerebrovascular accidents and never with gliomas.

The location of both presumed cerebrovascular accidents and gliomas was consistent with the literature with most presumed cerebrovascular accidents were in the

cerebellum, thalamus, caudate nucleus, and midbrain, whereas most gliomas were in the cerebrum.^{1,4-7,10}

When DWI was used in the group of presumed cerebrovascular accidents, five of the nine presumed cerebrovascular accidents were hyperintense in DWI and hypointense on ADC maps, consistent with cytotoxic edema and reduced Brownian motion of the water molecules (Fig. 3).^{17,20,21} One dog imaged 6 days after onset of clinical signs had isointense signal in DWI and hyperintense signal on ADC maps and one dog imaged 1 day after onset of clinical signs had mixed intensities in DWI and on ADC maps. In humans, patients who reperfuse early demonstrate a more rapid rise in ADC values and a significant amount of heterogeneity in the ADC values within the ischemic area.¹⁷ Early reperfusion is the most likely explanation for the changes observed in DWI and ADC values in these two dogs. Two presumed cerebrovascular accidents were hyperintense on both DWI and ADC maps. These two dogs underwent MR imaging examination 1 and 2 days after acute onset of clinical signs and therefore would be expected to have a lesion that was hyperintense on DWI and hypointense on the ADC map. It is possible that very early reperfusion of the presumably infarcted area and early development of vasogenic edema could have lead to these hyperintensities on both DWI and ADC maps, reflecting increased water content with no decreased motion of water molecules. When DWI was used in dogs with gliomas, the majority of gliomas were hyperintense on both DWI and ADC maps (Fig. 4). This is consistent with a T2 shine-through effect, most likely due to necrosis, microcystic degeneration and hemorrhage, all typical of gliomas. None of the gliomas had high signal on DWI and low signal on ADC maps that could have lead to potential confusion with acute infarction. DWI was helpful in reaching a diagnosis in the dogs of this study. After evaluation of T2W and T1W sequences, 10–47% of presumed cerebrovascular accidents were misdiagnosed as gliomas and 0–12% of gliomas were misdiagnosed as cerebrovascular accidents. However, when DWI was added, the percentage of presumed cerebrovascular accidents misdiagnosed as gliomas decreased to 11–33% and none of the gliomas were misdiagnosed as cerebrovascular accidents. Clearly, DWI is valuable in distinguishing between a glioma and an infarct.

Ependymomas were not included in the glioma group. These tumors are derived from the lining epithelium of the ventricles, being most commonly located in the lateral ventricle and less commonly in the third or the fourth

ventricles. Because of their location, the diagnosis is usually more straightforward than for other gliomas and confusion with a cerebrovascular accident is unlikely.^{1,2,10}

Unfortunately, there was no histopathologic confirmation for the majority of dogs with presumed cerebrovascular accidents. To increase the number of dogs with presumed cerebrovascular accidents in our study, we included dogs with acute onset of nonprogressive signs of a brain lesion that were alive 1 year after imaging with improvement or no progression of clinical signs. Similar criteria have been used previously.^{4-7,13,14} A 1-year survival for dogs with presumed cerebrovascular accidents was selected to exclude the possibility of glioma; this exceeds the 0.2 month median survival for dogs with brain tumors treated symptomatically, including corticosteroids.²² In addition, a 1-year survival exceeds the 40.4 week (95% confidence interval 26.3–54.5 weeks) median survival of dogs with intraaxial tumors treated with radiation therapy and corticosteroids.²³ None of the dogs in our study received radiation therapy or other advanced treatment; therefore, supporting the exclusion of a glial tumor in our three dogs treated with corticosteroids that survived more than 1 year. However, we cannot rule out that some of the dogs with a presumed cerebrovascular accident had infectious or noninfectious inflammatory lesions, although spontaneous regression of such lesions is uncommon. Inflammatory and infectious brain lesions are more typically characterized by a fluctuating clinical course. By using this extended time frame and recording the improvement or nonprogression of the clinical signs, we tried to maximize the exclusion of possible inflammatory or infectious brain disease. And, narrowing the inclusion criteria for patients with histopathologically confirmed cerebrovascular accidents would have induced a selection bias for severely affected patients.

The observers were unaware of the history and signalment, in particular the duration of clinical signs. This may have affected the decision making between glioma and presumed cerebrovascular accidents. Finally, there was a lack of a standardized imaging protocol. Consistent use of sequences such as T2* gradient-echo, fluid-attenuation inversion recovery, and DWI may have helped characterize the lesions and could have improved the accuracy of the MR imaging diagnosis.

ACKNOWLEDGMENTS

The authors thank Melissa Sanchez for her assistance with histopathology in this study.

REFERENCES

1. Thomas WB, Wheeler SJ, Kramer R, Kornegay JN. Magnetic resonance imaging features of primary brain tumors in dogs. *Vet Radiol Ultrasound* 1996;37:20–27.
2. Kraft SL, Gavin PR, DeHaan C, Michael M, Wendling LR, Leathers CW. Retrospective review of 50 canine intracranial tumors evaluated by magnetic resonance imaging. *J Vet Intern Med* 1997;11:218–225.

3. Snyder JM, Shoefers FS, Van Winkle TJ, Massicotte C. Canine intracranial primary neoplasia: 173 cases (1986–2003). *J Vet Intern Med* 2006;20:669–675.
4. McConnell JF, Garosi L, Platt SR. Magnetic resonance imaging findings of presumed cerebellar cerebrovascular accident in twelve dogs. *Vet Radiol Ultrasound* 2005;46:1–10.
5. Garosi L, McConnell JF, Platt SR, et al. Clinical and topographic magnetic resonance characteristics of suspected brain infarction in 40 dogs. *J Vet Intern Med* 2006;20:311–321.
6. Berg JM, Joseph RJ. Cerebellar infarcts in two dogs diagnosed with magnetic resonance imaging. *J Am Anim Hosp Assoc* 2003;39:203–207.
7. Irwin JC, Dewey CW, Stefanacci JD. Suspected cerebellar infarcts in 4 dogs. *J Vet Emerg Crit Care* 2007;17:268–274.
8. Kraft SL, Gavin PR. Intracranial neoplasia. *Clin Tech Small Anim Pract* 1999;14:112–123.
9. Koestner A, Bilzer T, Schulman FY, Summers BA, Van Winkle TJ. Histological classification of tumors of the nervous system of domestic animals, Vol. 71. 2nd series. Washington, DC: Armed Forces Institute of Pathology, 1999.
10. Summers BA, Cummings J, deLahunta A. Tumors of the central nervous system. In: *Veterinary neuropathology*. St Louis, Missouri: Mosby Year Book Inc., 1995;362–376.
11. Platt SR, Garosi L. Canine cerebrovascular disease: do dogs have strokes? *J Am Anim Hosp Assoc* 2003;39:337–342.
12. Thomas WB, Sorjonen DC, Scheuler RO, Kornegay JN. Magnetic resonance imaging of brain infarction in seven dogs. *Vet Radiol Ultrasound* 1996;37:345–350.
13. Panarello GL, Dewey CW, Barone G, Stefanacci JD. Magnetic resonance imaging of two suspected cases of global brain ischemia. *J Vet Emerg Crit Care* 2004;14:269–277.
14. Timm K, Flegel T, Oechtering G. Sequential magnetic resonance imaging changes after suspected global brain ischemia in a dog. *J Soc Adm Pharm* 2008;49:408–412.
15. Rodenas S, Pumarola M, Gaitero L, Zamora A, Anor S. Magnetic resonance imaging findings in 40 dogs with histologically confirmed intracranial tumours. *Vet J* 2009, doi:10.1016/j.tvjl.2009.10.011.
16. Eck D. The Chi Square Statistic. Mathbeans Project, Department of Mathematics and Computer Science, Hobart and William Smith Colleges. Available at <http://math.hws.edu/javamath/ryan/ChiSquare.html> (accessed November 19, 2009).
17. Marks MP. Cerebral ischemia and infarction. In: Atlas SW (ed) *Magnetic resonance imaging of the brain and spine*. Philadelphia, PA: Wolters Kluwer, Lippincott Williams & Wilkins, 2009;772–825.
18. Jayaraman MV, Boxerman JL. Adult brain tumors. In: Atlas SW (ed) *Magnetic resonance imaging of the brain and spine*. Wolters Kluwer, Lippincott Williams & Wilkins, 2009;445–590.
19. Hervé D, Mangin J-F, Molko N, Bousser M-G, Chabriat H. Shape and volume of lacunar infarcts: a 3D MRI study in cerebral autosomal dominant arteriopathy with subcortical infarcts and leukoencephalopathy. *Stroke* 2005;36:2384–2388.
20. Mukherji SK, Chenevert TL, Castillo M. Diffusion-weighted magnetic resonance imaging. *J Neuroophthalmol* 2002;22:118–122.
21. Beauchamp NJ, Ulug AM, Pässe TJ, van Zijl PCM. MR diffusion imaging in stroke: review and controversies. *Radiographics* 1998;18:1269–1283.
22. Heidner GL, Kornegay JN, Page RL, Dodge RK, Thrall DE. Analysis of survival in a retrospective study of 86 dogs with brain tumors. *J Vet Intern Med* 1991;5:219–226.
23. Brearley MJ, Jeffery ND, Phillips SM, Dennis R. Hypofractionated radiation therapy of brain masses in dogs: a retrospective analysis of survival of 83 cases (1991–1996). *J Vet Intern Med* 1999;13:408–412.